# Quantification by random walk of the optical parameters of nonlocalized abnormalities embedded within tissuelike phantoms

**Victor Chernomordik, David Hattery, and Amir H. Gandjbakhche**

*Laboratory of Integrative and Medical Biophysics, National Institute of Child Health and Human Development, National Institutes of Health, Bethesda, Maryland 20892*

**Antonio Pifferi, Paola Taroni, Alessandro Torricelli, Gianluca Valentini, and Rinaldo Cubeddu**

*Istituto Nazionale Fisica della Materia-Department of Physics, Politecnico di Milano, Piazza Leonardo da Vinci, 32, I-20133 Milan, Italy*

Received November 29, 1999

We have extended a random-walk theory that uses time-dependent contrast functions to quantify the cross section and the corrected scattering and absorption coefficients of abnormal nonlocalized targets from time-of-flight (TOF) data obtained in time-resolved transillumination experiments. Experimental TOF's are used to show that this newly developed random-walk method is able to quantify the size and the optical properties of embedded nonlocalized targets in with an error rate of ≤25%. © 2000 Optical Society of America

*OCIS codes:* 100.1830, 170.6920, 170.3660.

Great enthusiasm exists in the biomedical optics community for use of nonionizing visible and infrared radiation to image biological targets, such as tumors that are hidden in optically thick, turbid tissues (see the reviews in Refs. 1 and 2). However, strong light scattering in tissue prevents optical techniques from achieving a spatial resolution comparable with that of x rays. Thus, for these techniques, quantification of the optical characteristics of the target becomes a critical requirement for clinical success.

We have devised a new methodology based on a random-walk theory[3] that uses time-dependent contrast functions to derive the optical properties and the size of an abnormal target [with the scattering and (or) absorption coefficients higher than those of the background] from time-of-flight data measured in time-resolved transillumination experiments.[4]

Our analysis differs from studies based on the perturbation analysis of diffusion approximation[5,6] in that we model the increased scattering in the abnormal target as a time delay. We show that for inclusions with similar dimensions in the $x$, $y$, and $z$ directions (e.g., spheres, cubes, or cylinders with height close to diameter) the optical contrast from increased scattering is proportional to the cross section of the inclusion (in the $z$ direction) instead of to its volume as modeled in the perturbation analysis.

The outline of the data analysis is as follows: Let us assume a time-of-flight measurement in which the intensity $I(x, \Delta t)$ is recorded at position $x$ for a set of $\Delta t$. To calculate time-dependent contrast functions from experimental data, we use, as a reference, the maximal detected intensity $I(x_0, \Delta t)$:

$$C(x, \Delta t) = \frac{I(x, \Delta t) - I(x_0, \Delta t)}{I(x_0, \Delta t)}. \tag{1}$$

For a relatively small (size $d_i \ll L$, where $L$ is the slab thickness), abnormally absorbing inclusion, we can represent the inclusion by a set of ${N_a}^3$ independent absorbers located on a cubic lattice with spacing $d_s = \sqrt{2}/{\mu_{sc}}^{(0)\prime}$, where ${\mu_{sc}}^{(0)\prime}$ is the transport-corrected scattering coefficient of the background. The contrast function is[4]

$$C_a(x, \Delta t) \approx \sum_{{N_a}^3} \eta_{\text{eff}} \frac{W(x, \Delta t)}{p(\Delta t)}, \tag{2}$$

where $p(\Delta t)$ is the probability that in the absence of the inclusion an injected photon will reach the detector with time delay $\Delta t$; $W(x, \Delta t)$ is the probability that a photon, having visited the inclusion, will reach the detector with time delay $\Delta t$; and $\eta_{\text{eff}}$ is the effective absorptivity of an elementary absorber[4]:

$$\eta_{\text{eff}} = \eta_0 \exp\left[-\frac{\Delta\mu_a {\mu_{sc}}^{(0)\prime} {d_i}^2}{2}\right] = \eta_0 \exp\left\{-\frac{\eta_0[{\mu_{sc}}^{(0)\prime} d_i]^2}{2}\right\}, \tag{3}$$

where $\eta_0 = \Delta\mu_a/{\mu_{sc}}^{(0)\prime}$, and $\Delta\mu_a = \mu_a - {\mu_a}^{(0)}$ is the perturbation of the absorption coefficient inside the inclusion with respect to the background. The exponential factor introduced on the right-hand side of Eq. (3) deals with the additional absorption that is due to nonlocalization (i.e., size) of the inclusion. The index of the exponent is equal to the product of the average number of RW steps inside the inclusion, $[{\mu_{sc}}^{(0)\prime} d_i]^2/2$, and the probability that because of this additional absorption a photon will be absorbed at any lattice point inside the inclusion, $\eta_0$.[4]

Increased scattering inside an inclusion results in an additional time delay[4]

0146-9592/00/130951-03$15.00/0 

$$\Delta\tau = \frac{d_i^2[\mu_{sc} - \mu_{sc}^{(0)\prime}]}{2c} = \frac{d_i^2 \Delta\mu_{sc}}{2c}; \quad (4)$$

so for a purely scattering inclusion the contrast is given by

$$C_{sc}(x, \Delta t) \approx \frac{1}{p(\Delta t)} \frac{dW(x, \Delta t)}{dt} \Delta\tau = d\tilde{W}(x, \Delta t)\Delta\tau. \quad (5)$$

$C_{sc}(x, \Delta t)$ depends on the slope of the point-spread function [i.e., the time derivative of $W(x, \Delta t)$]. Hence, as has been shown theoretically (see Fig. 2 of Ref. 4), the largest $C_{sc}(x, \Delta t)$ corresponds to the smallest available time delays $\Delta t$, where even a small increase in the delay $\Delta t$ has a considerable effect on the number of detected photons. However, for $\Delta t > \Delta t_{max}$ ($\Delta t_{max}$ corresponds to the maximum value of the point-spread function), the contribution from $C_{sc}(x, \Delta t)$ is negligible (this part of the data is used to estimate the perturbation that is due to a change in absorption). These different dependencies of the contrast on time delay $\Delta t$ were confirmed in experiments[7,8] and by the new data presented below. We already saw this difference in contrast behavior when we successfully quantified the characteristics of a relatively small inclusion embedded in a tissuelike solid phantom.[4] In that case, the contrast was simply proportional to the perturbation of the absorption coefficient, which is valid for relatively small targets.

Incorporation of Eq. (3) into our data analysis allows us to study larger inclusions. Moreover, in the present algorithm we take advantage of the whole dependence of the contrast function on time delay instead of using only a pair of data points, as we did before.

We used three sets of two-dimensional experimental data from the Politecnico di Milano to test our new theoretical considerations. In these experiments the source and the detector moved in tandem (in 2-mm steps) on the opposite sides of a rectangular turbid slab of thickness $D = 50$ mm. A single perturbing cylinder with increased scattering and (or) absorption, with its diameter equal to its length $l = 10$ mm, was located midway between the two faces of the slab. For all three phantoms, nominal optical properties of the background and the inclusion are presented in Table 1. $I(x, \Delta t)$ was obtained for each position of the detector. No photon data were provided for $\Delta t$ less than 500 ps (no ballistic or quasi-ballistic photons).

Parametric curve fitting of the experimental $I(x_0, \Delta t)$ by use of the theoretical expressions based on the RW model provided us with estimates of $\mu_{sc}^{(0)\prime}$ and $\mu_a^{(0)}$. To determine the center position of the inclusion inside the tissue slab and its effective dimensions, we used contrast scans for the shortest $\Delta t$. Assuming a cubic inclusion, represented by $N_a^3$ independent, identical elementary lattice points, we curve fitted the observed contrast (the fitting parameters were the effective absorptivity $\eta_{eff}$, the position of the inclusion center $r_i$, and the inferred effective distance $d_s$ between neighboring lattice sites in the target). $N_a$ was also an input parameter; however, the estimated physical dimensions of the inclusion $d_i = (N_a - 1)d_s$ did not change significantly with its variation. Theoretically, one should choose a value of $N_a$ that provides computed values of $d_s$ that are close to $d_s = \sqrt{2}/\mu_{sc}^{(0)\prime}$.[4]

Similar curve fitting with subsequent analysis of the behavior of $\eta_{eff}(\Delta t)$ was performed for a chosen set of time delays $\Delta t$. We expected that for relatively large time delays, $\Delta t > \Delta t_{max}$, the contribution of a scattering perturbation would be negligible, and $\eta_{eff}(\Delta t)$ should be constant.[4] In our model, $\eta_{eff}(\Delta t)$ of a purely absorbing inclusion should be almost constant. Among these three data sets, the one that has practically constant $\eta_{eff}(\Delta t)$ over the broad range of time delays corresponds to the target with insignificant scattering perturbation. For the other two data sets, $\eta_{eff}(\Delta t)$ increases rapidly with a decrease in $\Delta t$ if $\Delta t < \Delta t_{max}$, which indicates that the scattering properties of the inclusion differ significantly from those of the background. This result is consistent with the nominal values of the optical coefficients of the targets.

When values of $\mu_{sc}^{(0)\prime}$, $\eta_{eff}$, and $d_i$ are estimated from curve fitting, Eq. (3) can provide a numerical solution for the unknown parameter $\eta_0$, and, correspondingly, the magnitude of the absorption perturbation $\Delta\mu_a = \eta_0 \mu_{sc}^{(0)\prime}$. To find $\Delta\mu_a$, we should solve the modified Eq. (3):

$$\Phi(\eta_0) = |1 - \eta_{eff}/\eta_0 \exp\{\eta_0[\mu_{sc}^{(0)\prime} d_i]^2/2\}| = 0. \quad (6)$$

Note that the Eq. (6) has two roots, $\eta_1$ and $\eta_2$. Taking into account the size of the target, we have to choose the second root unless $\eta_2 N_a$ is greater than 1. This constraint corresponds to complete absorption in the RW analysis. Otherwise the value of the smaller first root, $\eta_1$, should be selected.

$\Delta\mu_{sc}'$ is determined by the average slope of $C_{sc}(x, \Delta t)$ as a function of $d\tilde{W}$ [see Eq. (4) and relation (5)]. In Fig. 1 the relationship between experimental contrast amplitude $C(\Delta t)$ and that calculated from the RW-theory value of $d\tilde{W}(\Delta t)$ is

**Table 1. Estimated Parameters for Three Inclusions**[a]

| | Background Optical Coefficients (Nominal/Reconstructed) | | Target Optical Coefficients (Nominal/Reconstructed) | | Target Size (Nominal/Reconstructed) |
|---|---|---|---|---|---|
| Target[b] | $\mu_{sc}^{(0)\prime}$ (mm$^{-1}$) | $\mu_a^{(0)}$ (mm$^{-1}$) | $\mu_{sc}'$ (mm$^{-1}$) | $\mu_a$ (mm$^{-1}$) | $d_I$ (mm) |
| I | 1.0/1.06 (6%) | 0.01/0.0093 (−7%) | 1.0/1.0 (0%) | 0.04/0.038 (−5%) | 10.0/12.2 (22%) |
| II | 1.0/1.06 (6%) | 0.01/0.0094 (−6%) | 2.0/2.5 (25%) | 0.01/0.0105 (5%) | 10.0/9.7 (−3%) |
| III | 1.0/1.06 (6%) | 0.01/0.0095 (−5%) | 1.0/2.28 (14%) | 0.04/0.034 (−15%) | 10.0/9.5 (−5%) |

[a]Errors are shown in parentheses.
[b]I, increased absorption; II, increased scattering; III, increased absorption and scattering.

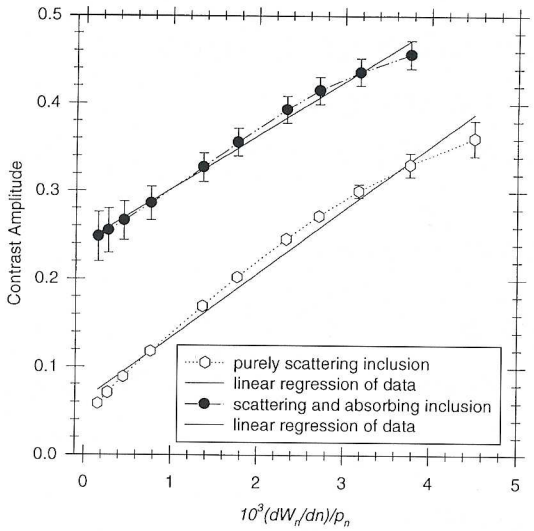


Fig. 1. Dependence of contrast on the derivative of the point-spread function for inclusions with increased scattering and with and without increased absorption (Milan data).

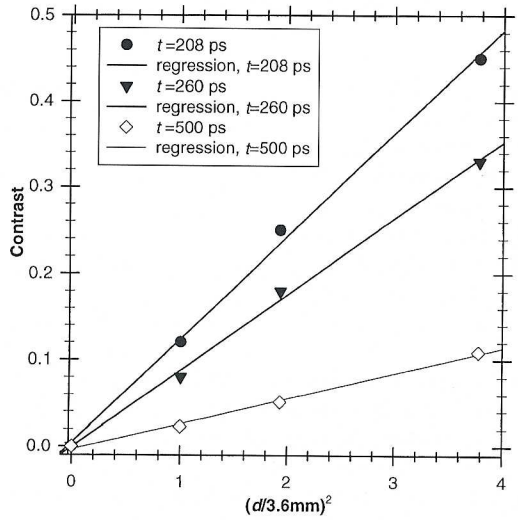


Fig. 2. Dependence of contrast on the squared size of scattering inclusion $d^2$ for different values of time delay (experimental data from Ref. 8).

presented for two inclusions. As expected, for short time delays ($\Delta t \leq 2000$ ps) the total contrast depends linearly on $d\tilde{W}$. The two inclusions, which have the same scattering perturbation, exhibit a similar slope; the offset in the first curve is due to absorption perturbation, which is absent for the second target.

The results of our analysis of three sets of Milan data are presented in Table 1. For each of the abnormal targets, the nominal values, the reconstructed values, and the percent error are shown. The reconstructed values are in good agreement with the nominal values: The nominal values have a 20% uncertainty in their magnitudes as reported by researchers at the Politecnico di Milano.

We tested the dependence of contrast amplitude on the size of the inclusion by using experimental data provided by Painchaud *et al.*[8] Time-resolved contrast functions for three similar, purely scattering inclusions that differ only in size ($d$ = 3.6, 5.0, 7.0 mm) were measured. In Fig. 2 we present experimental contrast amplitudes as a function of the squared size of the inclusion for three values of time delay. In all these cases the dependence proved to be very close to linear (and passed through the origin), as we expected from our model [see Eq. (4) and relation (5)]. Using our methodology, we were able to estimate $\mu_{sc}'$ inside the inclusion to be $\mu_{sc}' = 1.91\ \text{mm}^{-1}$, close to the nominal value of $\mu_{sc}' = 1.76\ \text{mm}^{-1}$.

We have successfully tested a new quantitative methodology that uses available time-of-flight measurements to reconstruct the optical properties of a nonlocalized abnormality embedded in an otherwise homogeneous, optically turbid background. Several improvements of the forward model have been discussed, in particular, the proportionality of the scattering contrast to the cross section of the target and an exponential correction factor for nonlocalized absotptive targets. Unless these two factors are taken into account, existing tomographic tools for diffuse photons can hardly be used for quantification of tissue abnormalities. The remaining challenge is to devise a similar methodology for the case when the background is not perfectly homogeneous. It should be noted, however, that large variations in the background's optical properties could mask the contrast that results from the target to be imaged. Thus the alternative is to work at wavelengths at which fluctuations of the optical signal that are due to background heterogeneity are much less than that of the contrast that results from the abnormal target.

A. H. Gandjbakhche's e-mail address is amir@helix.nih.gov.

## References

1. J. C. Hebden, S. R. Arridge, and D. T. Delpy, Phys. Med. Biol. **42,** 825 (1997).
2. S. R. Arridge and J. C. Hebden, Phys. Med. Biol. **42,** 841 (1997).
3. A. H. Gandjbakhche and G. H. Weiss, in *Progress in Optics*, E. Wolf, ed. (Pergamon, London, 1995), Vol. 34, p. 333.
4. A. H. Gandjbakhche, V. Chernomordik, J. C. Hebden, and R. Nossal, Appl. Opt. **37,** 1973 (1998).
5. J. C. Hebden and S. R. Arridge, Appl. Opt. **35,** 6788 (1996).
6. Y. Painchaud, A. Mailloux, M. Morin, S. Verreault, and P. Beaudry, Appl. Opt. **38,** 3686 (1999).
7. R. Cubeddu, A. Pifferi, P. Taroni, A. Torriceli, and G. Valentini, Appl. Opt. **35,** 4533 (1996).
8. Y. Painchaud, M. Morin, A. Mailloux, and P. Beaudry, Proc. SPIE **3597,** 556 (1999).